FEDSM2020-12388

DRAFT: THE EFFECT OF VARIYING VISCOSITY IN TURBULENT CHANNEL FLOW

Victor Coppo Leite
Ken and Mary Alice Lindquist
Department of Nuclear Engineering
Pennsylvania State University
State College, PA 16801
Email: vbc5085@psu.edu

Elia Merzari
Ken and Mary Alice Lindquist
Department of Nuclear Engineering
Pennsylvania State University
State College, PA 16801
Email: ebm5153@psu.edu

ABSTRACT

In various applications in nuclear engineering and in particular in test reactors, heat removal is carried by single-phase axial flow. In these applications, we observe sharp changes in molecular viscosity while the density presents very limited changes. As a consequence, the Reynolds number increases often by 2-3 folds across the channel, with an inlet value often transitional. In these conditions, turbulence changes significantly across the length of the channel with redistribution and thinning of the boundary layers. This is different from acceleration as the effect of changes in density is negligible. We aim to characterize in detail this phenomenon.

In particular Nek5000, a spectral-element computational fluid dynamics (CFD) code, will be used to perform DNS of fluid flow in the transition regime for channel flow with varying viscosity. We set up a novel benchmark case: the channel is extended in the stream-wise direction up to 20pi. The viscosity is kept constant in the first 4pi region. This inlet region is used as a cyclic region to obtain a fully developed flow profile at the beginning of the ramping region. The ramping region (4pi -20pi) is defined as a transition region where the viscosity is linearly decreased along the channel. The flow is homogenous in the span-wise direction due to the periodic boundary conditions. Due to the cyclic and wall boundary conditions, the flow is non-homogenous in the stream-wise and wall-normal direction respectively.

In this study, specific focus is given to the investigation of turbulence properties and structures in the near-wall region along the flow direction. Detailed turbulence budgets are collected and investigated. As expected, the results show that variation in the Reynolds across a channel does not cause an immediate change in the size of turbulent structures in the ramp region and a delay is in fact observed. Moreover, the results from the present study are compared with a correlation available in the literature for the friction velocity and as a function of the Reynolds-number.

NOMENCLATURE
A   You may include nomenclature here.
ν Viscosity.
x Streamwise direction.
y Vertical direction.
z Spanwise direction.
Re Reynolds number.
Re_τ Friction Reynolds number.
DNS   Direct Numerical Simulation.
ANL   Argonne National Laboratory.
τ_w Shear stress at the wall.
u_τ Friction velocity.
Re_τ Friction Reynolds number.
δ Height of the turbulence channel.
F_{Ci} Delayed function of Cases i=I,II and III.
a Viscosity linear coefficient.
R Relaxing parameter.
C Contractioning parameter.
δ_i Streamwise position where Region i starts, i=I,II and III.
Λ Signal contribution in the delayed function.
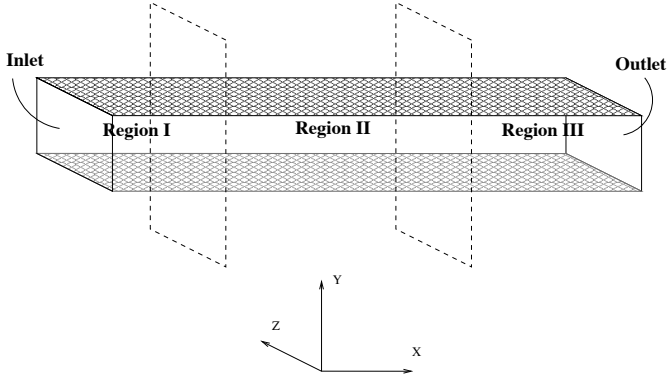
FIGURE 1: Geometry of the turbulence channel, the channel is divided into three different Regions.

BLABLABLA   Bullshit.

α There are two arguments for each entry of the nomemclature environment, the symbol and the definition.

The spacing between abstract and the text heading is two line spaces. The primary text heading is boldface in all capitals, flushed left with the left margin. The spacing between the text and the heading is also two line spaces.

INTRODUCTION

A schematic of the turbulence channels simulated are shown in Fig. 1. In this figure, Regions I, II and III are defined by two planes crossing the channel. A cycling region is implemented within Region I, Fig. 2. In this problem, the viscosity ν is a function of x, i.e., the streamwise distance. This parameter has constants values of $1E-4$ Pa.s and $5E-5$ Pa.s along Regions I and III respectively, while in region II it decreases with respect to the inverse of x.

In the present work, three cases varying the length of Region II are studied. Cases I, II and III have their Region II length of respectively 16π, 8π and 4π. Fig. 3 shows the plot of the viscosity as a function of x for each one of these cases and Fig. 4 shows the plot of the Reynolds number for them.

For all three Cases the inleat flow in Region I is considered to be fully developed with $Re_\tau = 550$, i.e., the same conditions as in [1]. Periodic condition is considered for the boundaries of the spamwise direction, i.e., z axis, and finally wall conditions are considered for the boudaries of the vertical direction, i.e., y axis.

METHODS - DIRECT NUMERICAL SIMULATION

In order to resolve the finest turbulent scales, the calculations of this work has been developed through Direct Numerical Simulation (DNS). To do so Nek5000 was employed, a spectral
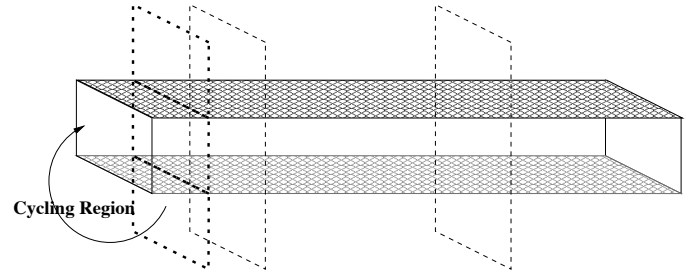

FIGURE 2: Cyclic region in the inlet.
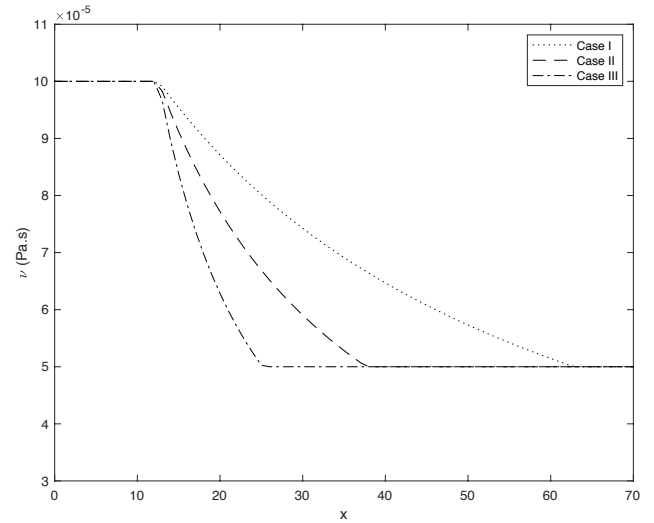
FIGURE 3: The viscosity of the considered Cases as a function of x.

element code developed in Argonne National Laboratory (ANL). Nek5000 has been validated in references [2] and [3].

The solution of this method is given by trigonometric series, in each element a polynomial functions of up to the twelveth degree have been employed to discretize the velocity field. Fig. 5 shows an example of the grid from half of the channel's cross section. One should notice that the discretization presented by this particular area is identical through all model's domain and it is only presented half of the cross-section for better visualization of the frame.

DNS simulations are able to simulate the finest turbulent length scales without using any turbulent model. Since the present work is focused on studying the contribution of the smaller scales to the energy cascade, it is required to use DNS rather than Reynolds Average Navier-Stokes (RANS) or Large Eddy Simulations (LES), although there is a substantial growth of the computational cost.

Copyright © 2020 by ASME
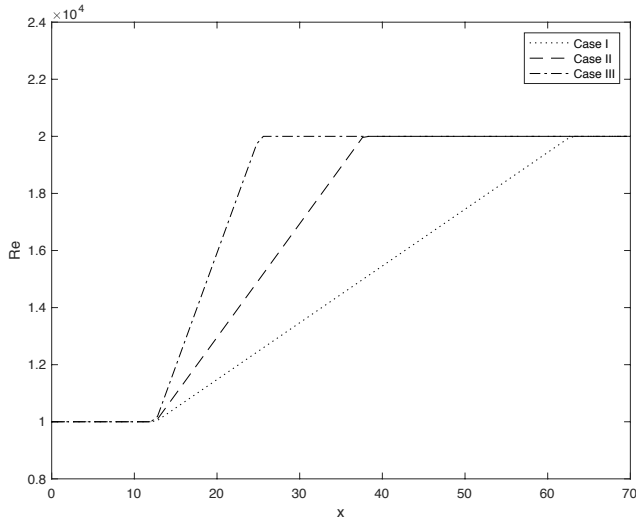
FIGURE 4: The Reynolds number as a function of the *x* for the considered Cases.
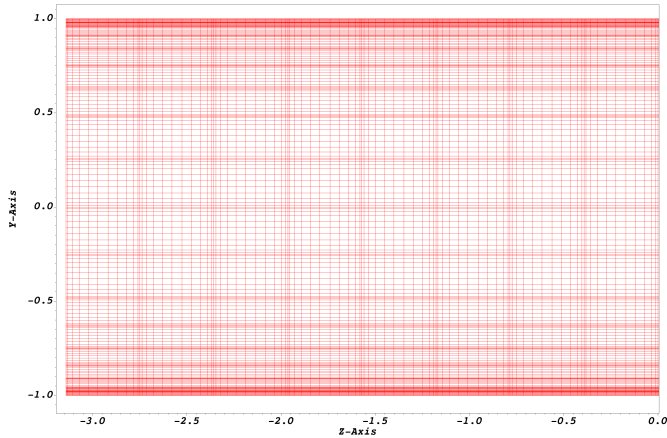
FIGURE 5: The grid employed in the simulation from half of the channel's cross section.

METHODS - CONVOLUTION ANALYSIS OF THE FRICTION REYNOLDS NUMBER

The friction Reynolds number has been calculated via numerical simulations for Cases I, II and III and this result was compared to the values obtained using an existed expression from Ref. [4] valid for fully developed turbulent flows. A delay in space can be seen between Re_τ when comparing the simulations' results with the values yielded from the mentioned expression. This way, these results are treated as signals in the space and a convolution operation is performed over the analytical expression for fully developed turbulent flows in order to built a

function that matches with the obtained values from the simulations.

To calculate the friction Reynolds number from the simulations several velocities profiles along *x* were obtained from the results and the viscous stress $\frac{d<U>}{dy}$ for these locations are calculated. Such values can then be applied in the set of definitions given from Eqn. 1 to Eqn. 3 following presented in order to calculate Re_τ.

$$\tau_w = \rho \nu \left(\frac{d<U>}{dy} \right)_{y=0} \tag{1}$$

Where ρ is the density and τ_w is the shear stress at the wall.

$$u_\tau = \sqrt{\frac{\tau_w}{\rho}} \tag{2}$$

Where u_τ is the friction velocity. And finally,

$$Re_\tau = \frac{u_\tau \delta}{\nu} \tag{3}$$

Where δ is the height of the simulated channels. For all Cases studied here this is a constant parameter $\delta = 2$.

The friction Reynolds number calculated using Eqn. 3 with the numeric simulations' results is then compared with Eqn. 4 from Ref. [4], which is valid for fully developed turbulent flows.

$$Re_\tau = 0.09 Re^{0.88} \tag{4}$$

The Reynolds numbers used to supply Eqn. 4 are those varying through *x* from Cases I, II and III, as presented in Fig. 4. The convolution to be performed over Eqn. 4 is given by Eqn. 5. In this equation $Re(\chi)$ stands for the analytical approximation given by Eqn. 4, $g(x - \chi)$ is a shifting function and χ is simply a dummy variable for the streamwise distance.

$$F(x) = \int_{-\infty}^{+\infty} Re_\tau(\chi) g(x - \chi) d\chi \tag{5}$$

As mentioned earlier, the simulated channels in the present study are divided in three Regions, as shown in Fig. **??** and a delayed function is built for each one of those. Since there is

no delay in Region I, no special treatment is required for it, thus $F(x) = Re_\tau(x) = 550$. Differently, in Region II and III the results from the numerical experiments are delayed when compared to those from Eqn. 4 and because of that a convolution operator takes place. Since we are dealing with a delayed signal in both Regions, a decaying exponential has been used as a shifting function, as proposed in Ref. [5].

In Region II, the friction Reynolds number is a linear function given by Eqn. 6.

$$Re_\tau(x) = ax + 550 \tag{6}$$

Where a is the linear coefficient of the increasing viscosity for each one of the three cases in Region II. Using Eqn. 6 in conjunction to the definition from Eqn. 5, one may derive Eqn. 7, which is the delayed function valid for Region II of the considered Cases.

$$F(x) = \frac{a}{R^2}(e^{-R(x-\delta_{II})} - 1) + \frac{a}{R}(x - \delta_{II}) + 550 \tag{7}$$

Where δ_{II} is the streamwise position that Region II starts and R is named relaxing parameter and it stands for the exponential decaying constant to be used in the shifting function $g(x - \chi)$ when dealing with Region II.

Eqn. 8 is the delayed function yielded applying Eqn. 5 over Region III, where a constant friction Reynolds number Re_τ predicted by Eqn. 4 takes place.

$$F(x) = (20000 - \Lambda)(1 - e^{-C(x-\delta_{III})}) + \Lambda \tag{8}$$

In this equation δ_{III} is the streamwise position that Region III starts, C is named contractioning parameter and it stands for the exponential decaying constant to be used in the shifting function $g(x - \chi)$ when dealing with Region III and finally $\Lambda = \frac{a}{R^2}(e^{-R(\delta_{III}-\delta_{II})} - 1) + \frac{a}{R}(\delta_{III} - \delta_{II}) + 550$, represents the contribution from Regions II to the delayed signal in Region III.

In summary, Eqn. (9) express the delayed function for Re_τ over the different Regions of the turbulence channels in the present work.

$$F(x) = \begin{cases} 550 & \text{(Region I)} \\ \frac{a}{R^2}(e^{-R(x-\delta_{II})} - 1) + \frac{a}{R}(x - \delta_{II}) + 550 & \text{(Region II)} \\ (20000 - \Lambda)(1 - e^{-C(x-\delta_{III})}) + \Lambda & \text{(Region III)} \end{cases} \tag{9}$$
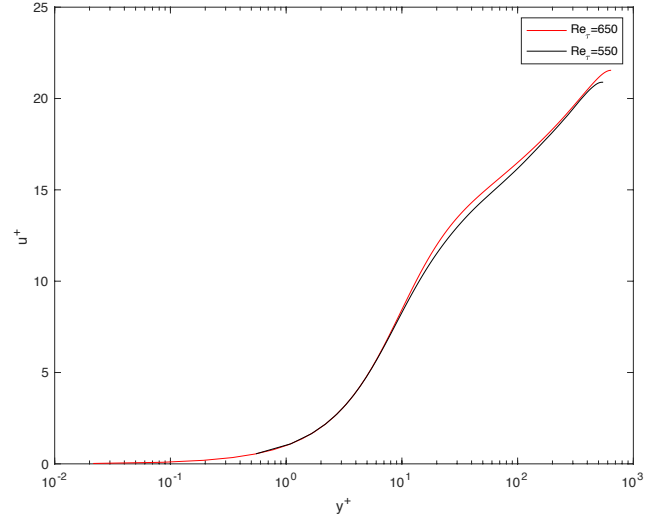
FIGURE 6: Comparing u^+ from Region I in Case I with already existed data in Ref [6].

FIGURE 7: Comparing $< uu >$ from Region I in Case I with already existed data in Ref [6].

RESULTS

The results from the three Cases considered in the present work are presented in this section. First, a comparison between the results in Region I from Case I with an existed data from Ref [6] is done in order to verify the model. Second, Re_τ results obtained via numerical models, through Eqn. 4 and by the derived delayed function $F(x)$ are presented. Third, the results
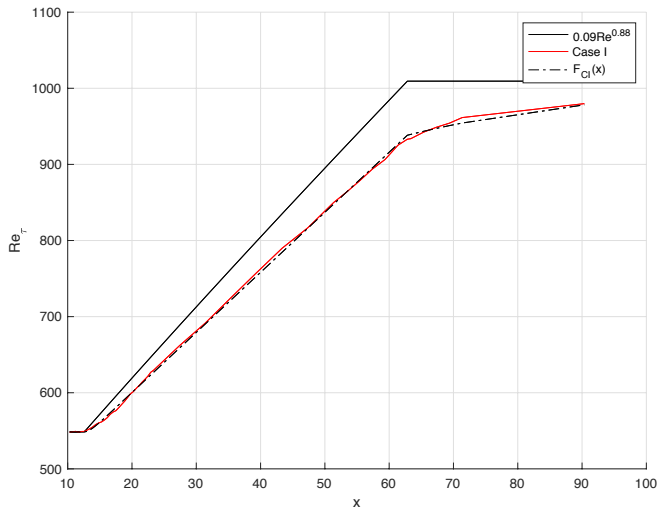
Model verification
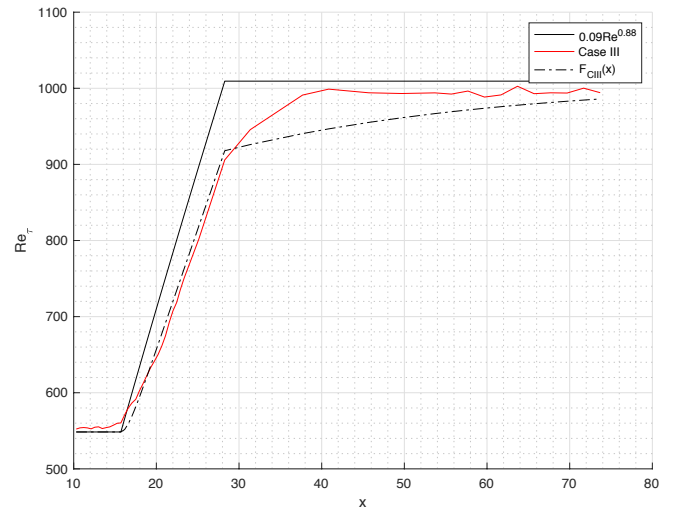**Turbulent structures**
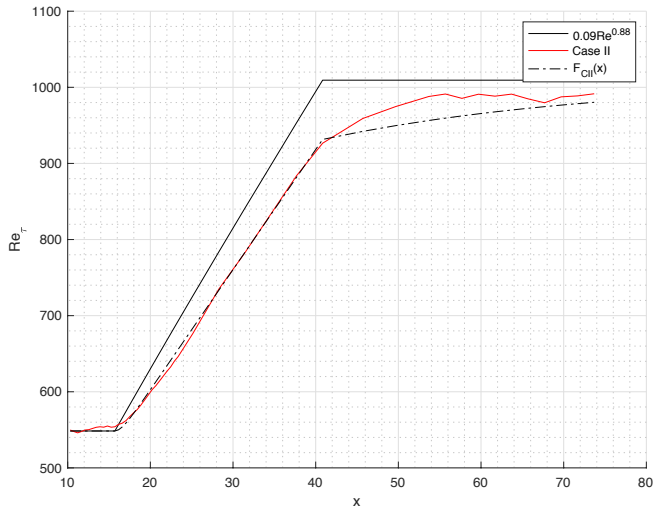**CONCLUSIONS**
ACKNOWLEDGMENT

REFERENCES

[1] Hoyas, S., and Jimenez, J., 2008. "Reynolds number effects on the reynolds stress budgets in turbulent channels". *Physics of Fluid,* **20**, October, p. 101511.
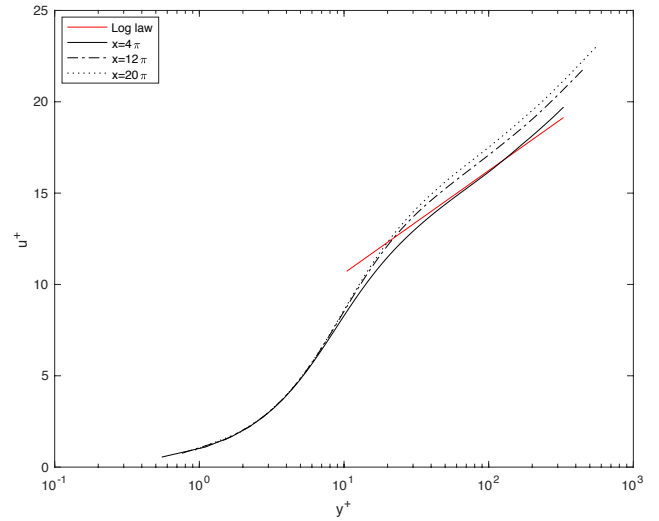
FIGURE 8: Friction Reynolds number through *x* for Case I.

**FIGURE 10**: Friction Reynolds number through *x* for Case III.

FIGURE 9: Friction Reynolds number through *x* for Case II.


FIGURE 11: u^+ versus y^+ obtained from Case I at $x = 4\pi$ (end of Region I), $x = 12\pi$ (middle of Region II) and $x = 20\pi$ (end of Region II) compared to the log law.

[2] Merzari, E., Pointer, W. D., and Fischer, P., 2013. "Numerical Simulation and Proper Orthogonal Decomposition in a Counter-Flow T-Junction". *Journal of Fluids Engineering, 135*, September, p. 091304.

[3] Obabko, A., Fischer, P., and Tautges, T., 2011. CFD Validation in OECD/NEA T-Junction Benchmark. Technical report 1, Argonne National Laboratory, Argonne, IL, June. See also URL http://www.osti.gov.

[4] Pope, S. B., 2000. *Turbulent Flows*. Cambridge University Press, New York.

[5] Oppenheim, A. V. Signals and systems. On MIT OpenCourseWare. URL http://ocw.mit.edu.

[6] Iwamoto, K., 2002. Database of Fully Developed Channel Flow, THTLAB Internal Report. Progress report ILR-0201, Dept. of Mech. Eng., The Univ. of Tokyo, Bunkyo-ku, Tokyo 113, June. See also URL http://thtlab.jp/DNS/CH12__PG.WL10.
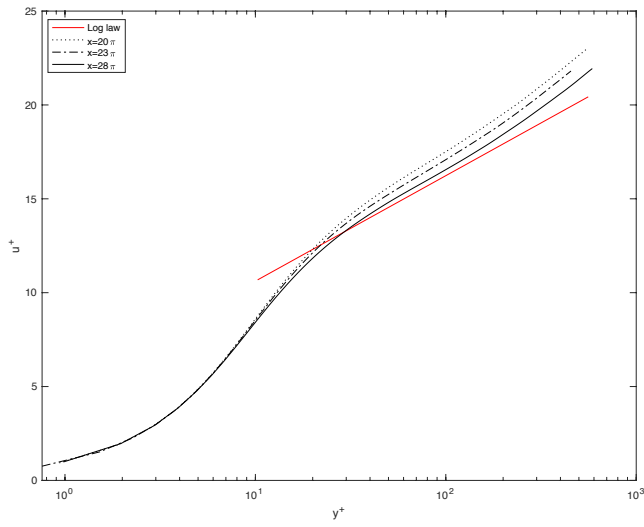
FIGURE 12: u^+ versus y^+ obtained from Case I at $x = 20\pi$ (end of Region I), $x = 23\pi$ (Region III) and $x = 28\pi$ (Region III) compared to the log law.
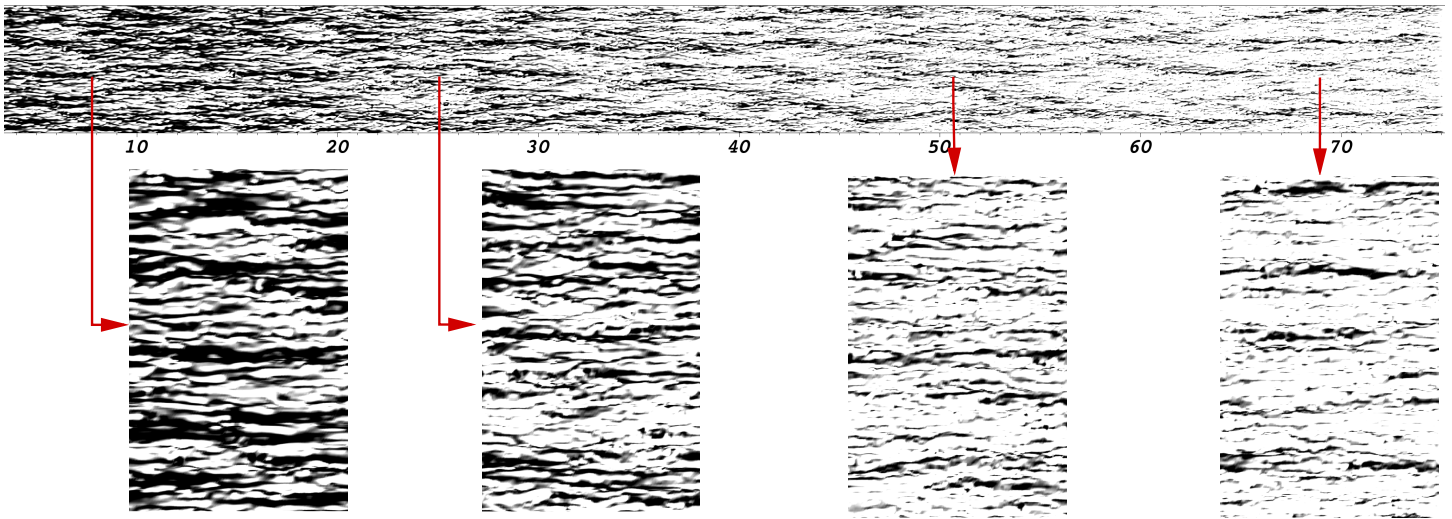
FIGURE 13: A cross section of the instantaneous streamwise velocity field at 0.01 from the wall.